

## Liquid–Liquid Critical Behavior of the {[bmim][BF<sub>4</sub>]/Triton X100 + Cyclohexane} Microemulsion

Hui H. Lü,<sup>†</sup> Xue Q. An,<sup>\*,‡</sup> and Wei G. Shen<sup>†,‡</sup>

<sup>†</sup>Department of Chemistry, Lanzhou University, Lanzhou, Gansu, 730000, China

<sup>‡</sup>Department of Chemistry, East China University of Science and Technology, Shanghai, 200237, China

**ABSTRACT:** The critical behavior of an ionic liquid-in-oil (IL-O) microemulsion of 1-butyl-3-methylimidazolium tetrafluoroborate [bmim][BF<sub>4</sub>] (IL), cyclohexane, and the nonionic surfactant polyoxyethylene *tert*-octylphenyl ether (T-X100) was studied for the first time. The coexistence curves of ( $T, n$ ) and ( $T, \Phi$ ) ( $n$  and  $\Phi$  are refractive index and volume fraction of the fraction of the volume of IL and T-X100 to the total volume of the system, respectively) for an IL-O microemulsion at constant pressure and a constant molar ratio ( $\omega$ ) of IL to T-X100 have been determined by measurements of the refractive index. The critical exponent  $\beta$  was deduced precisely from ( $T, n$ ) and ( $T, \Phi$ ) coexistence curves. These values were 0.329 and 0.330, respectively, and were consistent with the 3D Ising exponent within experimental uncertainties. The refractive index ( $n$ ) is a better choice of the concentration variable than the volume fraction ( $\Phi$ ) used for the construction of the order parameter to fit the Ising behavior.

### INTRODUCTION

Room temperature ionic liquids (ILs) are an interesting class of tunable solvents with essentially zero volatility. ILs are composed of sterically mismatched ions that hinder crystal formation; their molecular structure can be used to tune physicochemical properties. Their unique solvent properties are comparable with those of highly polar solvents, and they have already found uses in synthesis and catalytic reactions.<sup>1</sup> Despite these features, solubility limitations for apolar solutes remain, which could be overcome by the incorporation of hydrocarbon domains provided by formation of ionic liquid-in-oil (IL-O) microemulsion. The significance is that nanostructured surfactant assemblies would provide hydrophobic or hydrophilic nanodomains, thereby expanding potential applications of ILs as reaction, separation, and extraction media. Recently, Eastoe et al. have proved that the formation of IL-O microemulsions in mixtures of [bmim][BF<sub>4</sub>] (IL) and cyclohexane, stabilized by the nonionic surfactant polyoxyethylene *tert*-octylphenyl ether (T-X100).<sup>2</sup> Sequentially, a number of ionic liquid microemulsions have been proved.<sup>3–8</sup> Applications of these ionic liquid microemulsions, such as preparations of nano materials,<sup>9</sup> chemical reactions,<sup>10,11</sup> and selective extraction,<sup>12</sup> have also been reported.

Microemulsion systems exhibit complex phase behaviors in their phase diagrams, and the phase behaviors will provide important information for the potential applications of ILs microemulsion. At constant temperature and pressure, a phase diagram of a ternary mixture usually can be represented in a triangle, the corners of which represent the different components. If the temperature is also varied, an axis perpendicular to the plane of the triangle has to be introduced to depict the temperature dependence. The three-component mixtures of [bmim][BF<sub>4</sub>] (IL), polyoxyethylene *tert*-octylphenyl ether (T-X100), and cyclohexane can form IL-O microemulsion. An upper critical temperature ( $T_c$ ) was observed, and below  $T_c$  the mixture separates into two microemulsion phases of different

composition but with the same molar ratio  $\omega$  of [IL]/[T-X100]. Such a microemulsion system can be regarded as a pseudobinary mixture.<sup>13</sup> Therefore, the phase behavior can be depicted in a two-dimensional diagram with the concentration of droplets along the abscissa and temperature along the ordinate. A coexistence curve of temperature  $T$  against a concentration variable, such as volume fraction, can then be drawn in the same way as it was done for binary mixtures.<sup>13</sup> Refractive index measurements of coexisting phases are widely used in the study of critical phenomena, which was used as order parameter to describe the critical scaling behavior.<sup>13–20</sup>

The phase equilibrium for IL solution<sup>21–28</sup> and IL microemulsion<sup>29,30</sup> were reported. The critical behaviors as special phase behavior are of considerable interest since controversy from experiments and theories was raised about if these systems near the critical points belonged to the 3D Ising universality class.<sup>13,31–35</sup> The critical behaviors of the IL binary solutions also have been studied recently.<sup>36–40</sup> However, critical phenomena of the IL-O microemulsion have not been reported up to the present, so one does not realize if the critical behavior belong to the 3D Ising universality class.

Furthermore, the principle of universality predicts that sufficiently close to the critical point the various thermodynamic properties of liquids and liquid mixtures are governed by universal functions of the difference between the temperature and the critical temperature.<sup>41</sup> The critical effects in chemical reaction rates near a consolute point of the ordinary binary liquid systems have been reported for the test of the applicability of the principle of universality to reaction kinetics.<sup>42–45</sup> Therefore, it is also very important to obtain the critical properties of the new system (such as IL microemulsions) for studies of the kinetics of critical phenomena.

**Received:** September 18, 2010

**Accepted:** January 6, 2011

**Published:** February 02, 2011

In this work, we present a precise coexistence curve of an IL-O microemulsion, consisting of nonionic surfactant T-X100, [bmim][BF<sub>4</sub>] (IL), and cyclohexane at constant pressure and a certain molar ratio of IL to T-X100 ( $\omega = [\text{IL}]/[\text{T-X100}]$ ) by the refractive index measurement for the first time. The experimental results are analyzed to determine the critical exponent  $\beta$  and the critical amplitude  $B$ .

## EXPERIMENTAL SECTION

**Materials and Instruments.** 1-Butyl-3-methylimidazolium tetrafluoroborate [bmim][BF<sub>4</sub>] with mass fraction purity of 99.0 % (no more than 0.01 wt % water determined by Karl Fischer titration) was purchased from Merck. The nonionic surfactant T-X100 with a stated mass fraction purity of 99.9 % was obtained from Amresco. Cyclohexane (mass fraction purity of 99.5 %) was provided from Shanghai Lingfeng Chemical Reagent Company. All of the reagents were used as received. The apparatus used for refractive index measurements in this work was described previously.<sup>13</sup>

**Preparation of Samples and Determination of the Critical Volume Fraction and Critical Temperature.** The critical volume fraction ( $\Phi_c$ ) of [ $\Phi(\text{IL}/\text{T-X100}) + (1 - \Phi)$  cyclohexane] for the pseudobinary mixtures, where the  $\Phi_c$  was defined as the volume fraction of the system with the critical composition, was approached by fixing the molar ratio  $\omega$  of IL to T-X100 ( $\omega = [\text{IL}]/[\text{T-X100}]$ ) and by adjusting the amounts of cyclohexane to achieve equal volumes of the two phases at a phase separate temperature.<sup>13–15</sup> A sample with the critical composition was prepared in a rectangular fluorometer cell provided with Teflon plug, and the phase-separation temperature was then carefully measured ( $T$  measurement scale refers to IPTS-90) and taken as the critical temperature  $T_c$ . It was observed that samples nominally of the same composition had different values of the critical temperature, and the difference was as much as 1 K. The drift of the critical temperature observed in the same composition in different batches might be due to the involvement of the dust in the air to some extent in the preparation of the sample, which may be like the common case in the AOT/water/alkane systems. However, it did not affect the final results, because only one sample was used throughout the measurements of the whole coexistence curve, and only the temperature difference ( $T_c - T$ ) was important in data reductions to obtain the critical parameters.<sup>13</sup>

**Measurements of Refractive Indices.** A sample with the critical composition was prepared in a rectangular fluorometer cell provided with a Teflon plug; the refractive indices of each coexisting phase for the sample with the critical composition were measured at constant pressure and various temperatures by using the standard method of “minimum deviation”.<sup>13–15</sup> Figure 1 shows a schematic diagram of the apparatus for measurement of the refractive index by the method of “minimum deviation”. The fluorometer cell was placed in a holder inside a water bath. The temperature in the bath was controlled to within  $\pm 3$  mK and monitored by a digital platinum resistance thermometer (2700, Keithley Instruments Ltd.). A 2 mW He–Ne laser was used as a light source. The screen, the water bath, the cell holder, and the laser were adjusted so that the laser beam was normal to all surfaces of screen and glass walls. The position of the angle of minimum deviation ( $\theta'$ ) was determined by rotating the cell to minimize the distance ( $L_1$ ) between two spots of incident and refracted beams projected on the screen, where  $\theta$  is the angle of minimum deviation in water bath,  $L_2$  is the distance

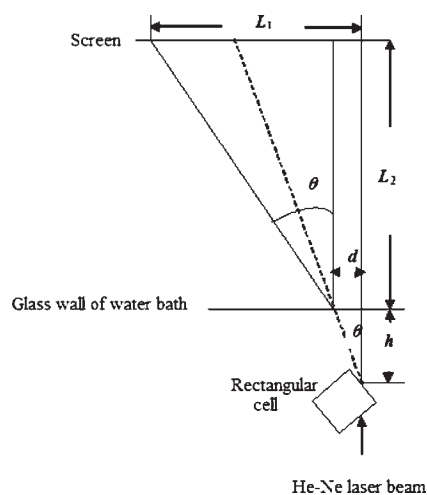


**Figure 1.** Schematic diagram of apparatus for measurement of the refractive index by the method of “minimum deviation”.

between the glass wall and screen,  $d$  is the distance between the spots projected with and without the rotated sample cell on the glass wall, and  $h$  is the distance between refracted spots on the rotated sample cell and the glass wall. The value of  $L_1$  was used to calculate the angle of minimum deviation by iteratively solving the following simultaneous equations:

$$(L_1 - d)/L_2 = \tan \theta' \quad (1)$$

$$d = h \tan \theta \quad (2)$$

$$n_a \sin \theta' = n_w \sin \theta \quad (3)$$

where  $n_a$  and  $n_w$  are the refractive indexes of air and water, respectively. The refractive index of the sample ( $n$ ) may then be obtained by

$$n = n_w [\sin(90^\circ + \theta)/2] / \sin 45^\circ \quad (4)$$

The refractive index is related to the density through the Lorentz–Lorenz formula:<sup>17</sup>

$$(n_2 - 1)/(n_2 + 2) = (4/3)\pi(\sum M_i \alpha_i / V) \quad (5)$$

where the sum is over all of the components of mass  $M_i$  and polarizability  $\alpha_i$ , and  $V$  is the volume of the components.

Continuous upward-slow shifts of phase-separation temperature near the critical point were observed. The rate of upward shifts was determined to be about  $0.001 \text{ K} \cdot \text{h}^{-1}$  by repeating measurements of critical temperature, and a correction was made to each observed temperature by subtraction of the shift value. Several measurements with the corrections in both heating and cooling modes were consistent within experimental uncertainties. During whole measurements the temperature difference ( $T_c - T$ ) was constant to  $\pm 0.001$  K. The uncertainty of measurement was about  $\pm 0.003$  K for temperature and  $\pm 0.0001$  for the refractive index.

## RESULTS AND DISCUSSION

As it was expected, upper critical points were observed for the IL microemulsion. The critical volume fraction  $\Phi_c$  of [ $\Phi(\text{IL}/\text{T-X100}) + (1 - \Phi)$  cyclohexane] and the critical temperature  $T_c$

for the microemulsion with  $\omega = 0.442$  were 0.229 and 304.034 K, respectively.

The refractive indices  $n$  of coexisting phases of the microemulsion were measured at a wavelength  $\lambda = 632.8$  nm and various temperatures. The results are listed in columns 2 and 3 of Table 1 and the coexistence curve of  $T$  against  $n$  shown in Figure 2a. In Table 1, the subscripts 1 and 2 represent the upper phase and lower phase for the microemulsion, respectively.

**Table 1. Coexistence Curves of the {[bmim][BF<sub>4</sub>]/T-X100 + Cyclohexane} Microemulsion with  $\omega = 0.442$  (Uncertainties in Measurements of  $T$  and  $n$  Are  $\pm 0.001$  K and  $\pm 0.0001$ , Respectively)<sup>a</sup>**

$(T_c - T)/K$	$n_1$	$n_2$	$\Phi_1$	$\Phi_2$
0.010	1.4312	1.4337	0.210	0.254
0.027	1.4310	1.4340	0.205	0.258
0.064	1.4305	1.4346	0.197	0.268
0.098	1.4301	1.4349	0.190	0.273
0.127	1.4300	1.4351	0.187	0.276
0.166	1.4298	1.4354	0.183	0.280
0.205	1.4295	1.4356	0.178	0.284
0.243	1.4294	1.4358	0.175	0.287
0.281	1.4293	1.4361	0.172	0.291
0.320	1.4292	1.4363	0.170	0.294
0.359	1.4290	1.4365	0.166	0.297
0.397	1.4289	1.4366	0.165	0.298
0.439	1.4288	1.4368	0.162	0.301
0.484	1.4287	1.4369	0.159	0.303
0.530	1.4285	1.4371	0.156	0.305
0.587	1.4284	1.4372	0.154	0.307
0.679	1.4283	1.4375	0.150	0.311
0.785	1.4281	1.4379	0.145	0.316
0.901	1.4279	1.4382	0.141	0.321
1.022	1.4278	1.4384	0.137	0.323

<sup>a</sup> Subscripts 1 and 2 represent the upper and lower phase;  $T$ ,  $n$ , and  $\Phi$  are the experimental temperature, the refractive index, and the volume fraction of the droplet, respectively;  $T_c = 304.034$  K.

To obtain the coexistence curve of  $T$  against  $\Phi$ , a series of ternary mixtures of {[bmim][BF<sub>4</sub>]/T-X100 + cyclohexane} with known volume fractions of the microemulsion were prepared, where  $\omega$  was fixed at 0.442. The refractive indices of these mixtures were measured in the one-phase region at various temperatures. The results are listed in Table 2. With the assumption that no significant critical anomaly is present in the refractive index, the refractive index of the microemulsion may be expressed as a linear function of temperature in a certain temperature range,<sup>13</sup>

$$n(\Phi, T) = n(\Phi, T^0) + (\partial n / \partial T)(T - T^0) \quad (6)$$

$$(\partial n / \partial T) = \Phi(\partial n_A / \partial T) + (1 - \Phi)(\partial n_B / \partial T) \quad (7)$$

**Table 2. Refractive Index  $n$  at a Wavelength  $\lambda = 632.8$  nm for the {[bmim][BF<sub>4</sub>]/T-X100 + Cyclohexane} Microemulsions with  $\omega = 0.442$  for Various Temperatures  $T$  and Volume Fractions of the Droplet  $\Phi$  (Uncertainties in Measurements of  $T$  and  $n$  Are  $\pm 0.001$  K and  $\pm 0.0001$ , Respectively)**

$\Phi$	$T/K$	$n$	$T/K$	$n$	$T/K$	$n$
0.000	301.069	1.4207	301.891	1.4203	303.280	1.4195
	300.321	1.4211	302.582	1.4199	304.013	1.4190
0.220	305.066	1.4310	306.950	1.4300	308.809	1.4290
	306.014	1.4305	307.925	1.4295	309.752	1.4285
0.224	304.117	1.4319	305.940	1.4309	307.754	1.4300
	305.003	1.4314	306.841	1.4305	308.633	1.4295
0.229	304.786	1.4320	307.163	1.4308	309.610	1.4295
	305.577	1.4316	308.015	1.4303	310.595	1.4290
0.250	301.913	1.4348	304.187	1.4336	306.260	1.4325
	303.071	1.4342	305.275	1.4330	307.391	1.4319
0.299	303.377	1.4369	305.005	1.4360	306.595	1.4352
	304.197	1.4365	305.853	1.4356	307.335	1.4348
0.340	301.476	1.4402	303.689	1.4391	305.703	1.4380
	302.567	1.4396	304.760	1.4385	306.651	1.4376
0.373	301.746	1.4423	303.233	1.4416	304.880	1.4408
	302.507	1.4419	304.016	1.4412	305.807	1.4403

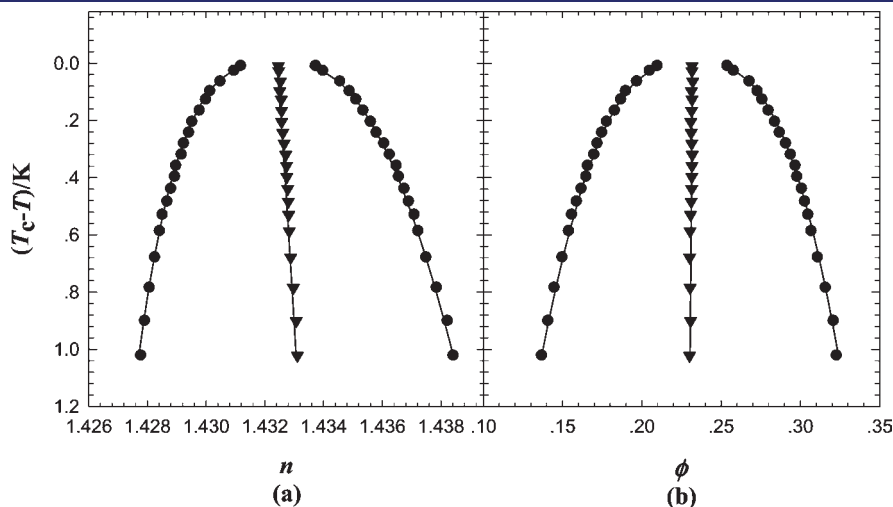


**Figure 2.** Coexistence curves of the {[bmim][BF<sub>4</sub>]/T-X100 + cyclohexane} microemulsion with  $\omega = 0.442$ : (a)  $T$  vs  $n$ ; (b)  $T$  vs  $\Phi$ ; ●, experimental values of concentration variables ( $\rho$ ) of coexisting phases; ▼, experimental values of diameter ( $\rho_d$ ) of the coexisting phases; the lines are concentration variables ( $\rho_{cal}$ ) and diameter ( $\rho_{d,cal}$ ) calculated from eqs 11, 12a, and 13 with coefficients listed in Tables 3 and 4.  $n$  and  $\Phi$  are the refractive index and volume fraction, respectively.

where  $T^0$  is chosen as 303.54 K (about the middle temperature of the coexistence curve determined in this work),  $(\partial n/\partial T)$  is the derivative of  $n$  with respect to  $T$ , and  $(\partial n_A/\partial T)$  and  $(\partial n_B/\partial T)$  represent the values of  $(\partial n/\partial T)$  for  $\Phi = 1$  and 0, respectively. Rearrangement of eqs 6 and 7 yields:

$$n(\Phi, T) = n(\Phi, T^0) + [\Phi(\partial n_A/\partial T) + (1 - \Phi)(\partial n_B/\partial T)](T - T^0) \quad (8)$$

The values of  $n(\Phi, T)$  listed in Table 2 were fit to eqs 7 and 8 to obtain  $(\partial n_A/\partial T) = -4.2 \cdot 10^{-4} \text{ K}^{-1}$ ,  $(\partial n_B/\partial T) = -5.6 \cdot 10^{-4} \text{ K}^{-1}$ , and  $n(\Phi, T^0)$ . We obtained the expression  $n(\Phi, T^0)$  as

$$n(\Phi, T^0) = 1.4208 + 0.0453\Phi + 0.0262\Phi^2 \quad (9)$$

The small standard deviation of 0.0002 in refractive index indicates that eq 9 is valid. The refractive indexes measured for the coexisting phases at various temperatures were converted to the volume fractions by simultaneously solving eqs 6, 7, and 9 by the Newton's iteration method using the soft of Sigmaplot 10.0, where the uncertainties of  $T$ ,  $n$ ,  $\Phi$ , and  $\Phi_c$  were estimated by the stability of temperature controlling, the differentiable distant of the refracted spot projected on the screen by naked eye, the converting from  $n$ , and the precision of the balance, respectively. This allowed us to simplify the procedure of determination of the dependence of  $n$  on  $\Phi$  just by fitting a polynomial form to  $n(\Phi, T^0)$  for various  $\Phi$  at  $T^0$ .

The values of the refractive index then were converted to volume fractions by calculating  $n(\Phi, T^0)$  through eq 8 and iteratively solving eq 9. The results are listed in columns 4 and 5 in Table 1 and shown in Figure 2b.

The difference of concentration variables  $(\rho_2 - \rho_1)$  may be expressed by the Wegner expression,

$$(\rho_2 - \rho_1) = B\tau^\beta + B_1\tau^{\beta+\Delta} + \dots \quad (10)$$

where  $\tau = (T_c - T)/T_c$ ,  $\beta$  and  $\Delta$ , are critical exponents,  $B_1$  is the amplitude of the first Wegner correction term,  $\rho$  is the concentration variable, and  $\rho_2$  and  $\rho_1$  are the values of  $\rho$  in the lower and upper coexisting phases, respectively. In the region sufficiently closed to the critical temperature, the simple scaling is valid:

$$(\rho_2 - \rho_1) = B\tau^\beta \quad (11)$$

It is well-known that a wrong choice of the variable may cause a significant reduction of the region of validity of eq 11. The values of  $\beta$  in different  $\tau$  regions for  $n$  and  $\Phi$  were estimated by fitting the experimental data to eq 11. Figure 3 shows the dependence of the value of  $\beta$  on the temperature range for the two choices of the order parameters, where the temperature range is represented by the cutoff value of maximum  $(T_c - T)$ , denoted by  $(T_c - T)_{\max}$  where the errors are the standard deviation for the fitting data of  $\tau$  and  $(\rho_2 - \rho_1)$  to eq 11. The results showed that the values of  $\beta$  depend on  $(T_c - T)_{\max}$  which increase slightly as the temperature range increased. The errors in determination of  $\beta$  increase as  $(T_c - T)$  is narrowed. This may result from the following reason: the critical fluctuate in the system is huge (and also the random of the components) when they are closed to the critical point. The phenomenon is also found in our previous studies. The values of  $\beta$  approach the 3D Ising value of 0.327 and are obviously inconsistent with the Fisher renormalized value of 0.365 and the mean theory value of 0.5 within experimental uncertainties in the region sufficiently

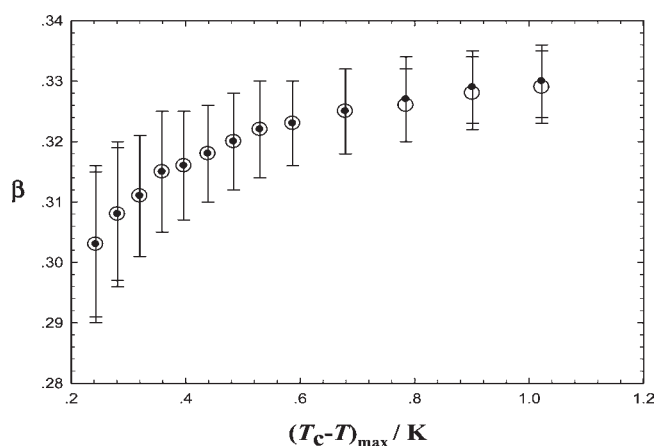


**Figure 3.** Plot of the critical exponent  $\beta$  in the difference range of  $(T_c - T)_{\max}$  obtained by fitting the experimental data to eq 10 for the {[bmim][BF<sub>4</sub>]/T-X100 + cyclohexane} microemulsion with  $\omega = 0.442$  for different order parameters:  $\circ$ , refractive index  $n$ ;  $\bullet$ , volume fraction  $\Phi$ .

close to the critical temperature for the two choices of variables  $n$  and  $\Phi$ . All of the experimental data were used to fit eq 11, and the values of  $\beta$  were obtained to be  $0.329 \pm 0.006$  and  $0.330 \pm 0.006$  for  $n$  and  $\Phi$ , respectively. Gao et al. have proved the small water content (1 wt % to 5 wt %) will make this IL-O droplet decrease.<sup>46</sup> However, the water in IL in our study is not more than 0.01 wt %, and the trace water effect can be neglected. The result indicated that this IL microemulsion may be taken as a pseudobinary mixture.

The goodness of variables used to construct the order parameters can also be tested by fitting the experimental data to eq 10 with fixed values of  $\beta = 0.327$  and  $\Delta = 0.5$  and by comparing the significance of the first Wegner correction. The critical amplitudes are listed in Table 3. The significance of the first Wegner correction term may be qualitatively indicated by the ratio of  $|B_1/B|$ . As shown in Table 3, the smaller values of  $|B_1/B|$  for order parameters  $n$  indicate that it may be slightly better choice than  $\Phi$  in this microemulsion system, and it is different from the AOT based microemulsions.<sup>13</sup>

The diameter of the coexistence curve may be expressed as,

$$\rho_d = (\rho_2 + \rho_1)/2 = \rho_c + A_0\tau + A_1\tau^{1-\alpha} + \dots \quad (12a)$$

otherwise, the diameter shows a  $2\beta$  anomaly:

$$\rho_d = (\rho_2 + \rho_1)/2 = \rho_c + A_0\tau + C\tau^{2\beta} + \dots \quad (12b)$$

We fit the experimental data to eqs 12a and 12b in separate fitting procedures with fixed values of  $\alpha = 0.11$  and  $\beta = 0.327$ ;  $\rho_c$ ,  $A_0$ ,  $A_1$ , and  $C$  are obtained, and the characteristics are summarized in Table 4. The experimental value of  $n_c$  was obtained by extrapolating the refractive index against temperature in the one-phase region to the critical temperature. The uncertainties of optimal parameters reported in Table 4 include no systematic ones contributed by converting  $n$  to  $\Phi$ . These uncertainties in  $\Phi_c$  were estimated to be  $\pm 0.001$ . Therefore, the values  $n_c$  and  $\Phi_c$  are consistent with the experimental results. This is evidence that no significant critical anomaly is present in refractive indices and the refractive indices were properly converted to volume fraction  $\Phi$ . Although eqs 12a and 12b omit the higher Wegner correction terms and artificially separate the effects of terms  $2\beta$  and  $(1 - \alpha)$ , comparing the standard deviations  $S$  and  $\rho_c$  in fitting eqs 12a and

**Table 3. Parameters in Equations 9 and 10 for Coexistence Curves ( $T, n$ ) and ( $T, \Phi$ ) for the {[bmim][BF<sub>4</sub>]/T-X100 + Cyclohexane} Microemulsion with  $\omega = 0.442$**

order parameters	$B$	$B_1$	$ B_1/B $
$n$	$0.067 \pm 0.001$		
	$0.064 \pm 0.001$	$0.083 \pm 0.015$	1.30
$\Phi$	$1.174 \pm 0.005$		
	$1.112 \pm 0.011$	$1.554 \pm 0.267$	1.40

**Table 4. Parameters of Equations 12a and 12b and Standard Deviations  $S$  in  $\rho$  for Diameters of Coexistence Curves of ( $T, n$ ) and ( $T, \Phi$ ) for the {[bmim][BF<sub>4</sub>]/T-X100 + Cyclohexane} Microemulsion with  $\omega = 0.442^a$**

	( $T, n$ )	( $T, \Phi$ )
$\rho_{c, \text{expt}}$	$1.4323 \pm 0.0001$	$0.229 \pm 0.001$
	$\rho_d = \rho_c + A_0\tau + A_1\tau^{1-\alpha}$	
$\rho_c$	$1.4324 \pm 0.0001$	$0.232 \pm 0.001$
$A_0$	$0.007 \pm 0.110$	$-0.818 \pm 1.836$
$A_1$	$0.102 \pm 0.059$	$0.184 \pm 0.990$
$S$	$2.1 \cdot 10^{-5}$	$3.5 \cdot 10^{-4}$
	$\rho_d = \rho_c + A_0\tau + C\tau^{2\beta}$	
$\rho_c$	$1.4324 \pm 0.0001$	$0.232 \pm 0.001$
$A_0$	$0.142 \pm 0.032$	$-0.577 \pm 0.540$
$C$	$0.008 \pm 0.005$	$0.015 \pm 0.079$
$S$	$2.1 \cdot 10^{-5}$	$3.5 \cdot 10^{-4}$

<sup>a</sup> $\rho_{c, \text{expt}}$  is the experimental critical value of the order parameter.

12b may give some indication of the significance of terms  $2\beta$  and  $(1 - \alpha)$ .

The combination of eqs 10 and 12a yields:

$$\rho_1 = \rho_c + A_0\tau + A_1\tau^{1-\alpha} + (1/2)B\tau^\beta + (1/2)B_1\tau^{\beta+\Delta} \quad (13)$$

$$\rho_2 = \rho_c + A_0\tau + A_1\tau^{1-\alpha} - (1/2)B\tau^\beta - (1/2)B_1\tau^{\beta+\Delta} \quad (14)$$

where  $\alpha$ ,  $\beta$ , and  $\Delta$  were fixed at 0.11, 0.327, and 0.5, respectively. The values of  $B$ ,  $B_1$ ,  $A_0$ ,  $A_1$ , and  $\rho_c$  were taken from Tables 3 and 4, and the values of  $\rho_1$ ,  $\rho_2$ , and  $\rho_d$  were calculated from eqs 12a, 13, and 14. The results are shown as lines in Figure 2.

We fixed the critical exponent  $\beta$  and  $\Delta$  at the theoretical values  $\beta = 0.327$  and  $\Delta = 0.5$ . A weighted nonlinear least-squares program was used to fit eq 10. The total uncertainties  $\sigma$  of  $\Delta\rho$  used in weighting were calculated by eq 15.<sup>33</sup>

$$\sigma^2 = [\sigma(\Delta\rho)]^2 + (B\beta\tau^{\beta-1}/T_c)^2 [\sigma(T_c - T)]^2 \quad (15)$$

where  $\sigma(\Delta\rho)$  and  $\sigma(T_c - T)$  are the uncertainties in measurements of  $\Delta\rho$  and  $(T_c - T)$ , respectively. The value of  $\sigma(\Delta\rho)$  is 0.0001 for  $\Delta n$  and 0.004 for  $\Delta\Phi$ . The residuals as a function of the temperature difference, which denotes the distance from the critical point, are shown in Figure 4. As can be seen, the errors between the experimental data and calculated one are in the range of the uncertainties of refractive index measurement and the  $\Phi$  converted by  $n$ .

## CONCLUSIONS

The coexistence curves of the IL-O microemulsion of {IL/T-X100 + cyclohexane} with a fixed molar ratio of 0.442

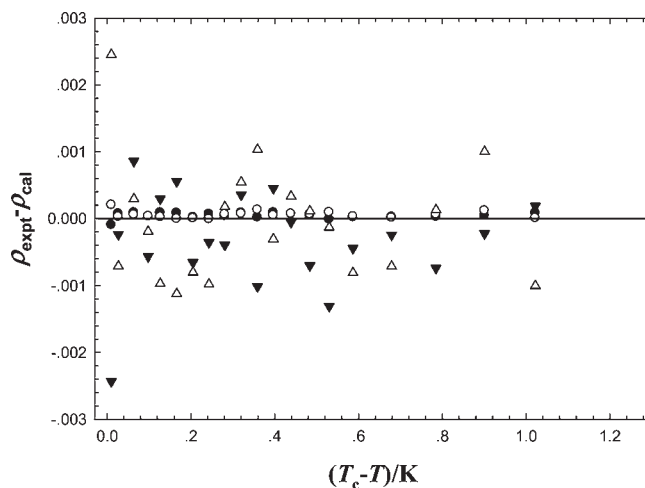


**Figure 4.** Plot of the residuals ( $\rho_{\text{expt}} - \rho_{\text{cal}}$ ) as a function of the temperature difference ( $T_c - T$ ) for coexistence curves of the {[bmim][BF<sub>4</sub>]/T-X100 + cyclohexane} microemulsion with  $\omega = 0.442$  for different order parameters:  $\bullet$ ,  $n_1$ ;  $\circ$ ,  $n_2$ ;  $\blacktriangledown$ ,  $\Phi_1$ ;  $\triangle$ ,  $\Phi_2$ , where  $\rho_{\text{expt}}$  is the experimental value,  $\rho_{\text{cal}}$  is calculated by eqs 12 and 13, and subscripts 1 and 2 represent upper and lower phases, respectively.

([IL]/[T-X100]) was determined in the critical region. It has been found that this system may be taken as a pseudobinary system; the values of critical exponent  $\beta$  of the microemulsion approach the 3D Ising value of 0.327 within the experimental uncertainties when the temperature is close to the critical point. The present studies confirm that the pseudobinary mixture of the microemulsion belongs to the 3D Ising universality class within the experimental uncertainties in the range of experimental temperature. The refractive index  $n$  is a better choice of the concentration variable than  $\Phi$  for constructing an order parameter.

## AUTHOR INFORMATION

### Corresponding Author

\*Tel.: +86-021-64250804, fax: +84-021-64250804, e-mail address: anxueqin@ecust.edu.cn.

### Funding Sources

This work is financially supported by the National Nature Science Foundation of China (Nos. 20673059, 20573056, and 21073063), the Nature Science Keystone Foundation of Shanghai (No. 08jc1408100), and the Fundamental Research Funds for the Central Universities, China (No. WK0913002).

## REFERENCES

- Zhao, D.; Wu, M.; Kou, Y.; Min, E. Ionic liquids: applications in catalysis. *Catal. Today* **2002**, *74*, 157–189.
- Eastoe, J.; Gold, S.; Rogers, S. E.; Paul, A.; Welton, T.; Heenan, R. K.; Grillo, I. Ionic liquid-in-oil microemulsions. *J. Am. Chem. Soc.* **2005**, *127*, 7302–7303.
- Gao, H. X.; Li, J. C.; Han, B. X.; Chen, W. N.; Zhang, J. L.; Zhang, R.; Yan, D. D. Microemulsions with ionic liquid polar domains. *Phys. Chem. Chem. Phys.* **2004**, *6*, 2914–2916.
- Gao, Y.; Li, N.; Zheng, L. Q.; Zhao, X. Y.; Zhang, S. H.; Han, B. X. A cyclic voltammetric technique for the detection of micro-regions of [bmim][PF<sub>6</sub>]/Tween 20/H<sub>2</sub>O microemulsions and their performance characterization by UV-Vis spectroscopy. *Green Chem.* **2006**, *8*, 43–49.
- Gao, Y.; Han, S. B.; Han, B. X.; Li, G. Z.; Shen, D.; Li, Z. H. TX-100/water/1-butyl-3-methylimidazolium hexafluorophosphate microemulsions. *Langmuir* **2005**, *21*, S681–S684.

- (6) Li, J.; Zhang, J.; Gao, H.; Han, B.; Gao, L. Nonaqueous microemulsion-containing ionic liquid [bmim][PF<sub>6</sub>] as polar microenvironment. *Colloid Polym. Sci.* **2005**, *283*, 1371–1375.
- (7) Gao, Y.; Zhang, J.; Xu, H. Y.; Zhao, X. Y.; Zheng, L. Q.; Li, X. W.; Yu, L. Structural studies of 1-butyl-3-methylimidazolium tetrafluoroborate/TX-100/p-Xylene ionic liquid microemulsions. *ChemPhysChem* **2006**, *7*, 1554–1561.
- (8) Rabe, C.; Koetz, J. CTAB-based microemulsions with ionic liquids. *Colloids Surf., A* **2010**, *354*, 261–267.
- (9) Zhang, G.; Zhou, H.; Hu, J.; Liu, M.; Kuang, Y. Pd nanoparticles catalyzed ligand-free Heck reaction in ionic liquid microemulsion. *Green Chem.* **2009**, *11*, 1428–1432.
- (10) Muhammad, M.; Kamiya, N.; Nakashima, K.; Goto, M. Water-in-ionic liquid microemulsions as a new medium for enzymatic reactions. *Green Chem.* **2008**, *10*, 497–500.
- (11) Li, X. W.; Zhang, J.; Zheng, L. Q.; Chen, B.; Wu, L. Z.; Lv, F. F.; Dong, B.; Tung, C. H. Microemulsions of N-alkylimidazolium ionic liquid and their performance as microreactors for the photocycloaddition of 9-substituted anthracenes. *Langmuir* **2009**, *25*, 5484–5490.
- (12) Shu, Y.; Cheng, D.; Chen, X.; Wang, J. A reverse microemulsion of water/AOT/1-butyl-3-methylimidazolium hexafluorophosphate for selective extraction of hemoglobin. *Sep. Purif. Technol.* **2008**, *64*, 154–159.
- (13) An, X.; Feng, J.; Shen, W. Critical behavior of a pseudobinary system for a three-component microemulsion. *J. Phys. Chem.* **1996**, *100*, 16674–16677.
- (14) An, X.; Shen, W.; Wang, H.; Zheng, G. The (liquid + liquid) critical phenomena of (a polar liquid + an n-alkane). I. Coexistence curves of (N,N-dimethylacetamide + hexane). *J. Chem. Thermodyn.* **1993**, *25*, 1373–1383.
- (15) Shen, W.; Smith, G. R.; Knobler, C. M.; Scott, R. L. Tricritical phenomena in bimodal polymer solutions. Three-phase coexistence curves for the system polystyrene (1) + polystyrene (2) + methylcyclohexane. *J. Phys. Chem.* **1990**, *94*, 7943–7949.
- (16) Andrew, W. V.; Khoo, T. B. K.; Jacobs, D. T. Testing the Lorentz–Lorentz Relation in the near-critical binary fluid mixture isobutyric acid and water. *J. Chem. Phys.* **1986**, *85*, 3985–3991.
- (17) Toumi, A.; Bouanz, M. Effect of the (K<sup>+</sup>, Cl<sup>-</sup>) ions on the order parameters and on Lorentz–Lorentz relation in the isobutyric acid-water critical mixture. *J. Mol. Liq.* **2005**, *122*, 74–83.
- (18) Venkatesu, P. Effect of polymer chain in coexisting liquid phases by refractive index measurements. *J. Chem. Phys.* **2005**, *123*, 024902–1–10.
- (19) Gutkowski, K. I.; Bianchi, H. L.; Japas, M. L. Critical behavior of a ternary ionic system: A controversy. *J. Chem. Phys.* **2003**, *118*, 2808–2814.
- (20) Bonetti, M.; Oleinikova, A.; Bervillier, C. Coexistence curve of the ionic binary mixture Ethylammonium nitrate-n-octanol: Critical properties. *J. Phys. Chem. B* **1997**, *101*, 2164–2173.
- (21) Arce, A.; Francisco, M.; Soto, A. Evaluation of the polysubstituted pyridinium ionic liquid [hmpy][Ntf<sub>2</sub>] as a suitable solvent for desulfurization: Phase equilibria. *J. Chem. Thermodyn.* **2010**, *42*, 712–718.
- (22) Wu, C. T.; Marsh, K. N.; Deev, A. V.; Boxall, J. A. Liquid-liquid equilibria of room-temperature ionic liquids and butan-1-ol. *J. Chem. Eng. Data* **2003**, *48*, 486–491.
- (23) Crosthwaite, J. M.; Aki, S. N. V. K.; Maginn, E. J.; Brennecke, J. F. Liquid phase behavior of imidazolium-based ionic liquids with alcohols. *J. Phys. Chem. B* **2004**, *108*, 5113–5119.
- (24) Maia, F. M.; Rodríguez, O.; Macedo, E. A. LLE for (water + ionic liquid) binary systems using [C<sub>x</sub>mim][BF<sub>4</sub>] (x = 6, 8) ionic liquids. *Fluid Phase Equilib.* **2010**, *296*, 184–191.
- (25) Abe, H.; Yoshimura, Y.; Imai, Y.; Goto, T.; Matsumoto, H. Phase behavior of room temperature ionic liquid – H<sub>2</sub>O mixtures: N,N-diethyl-N-methyl-N-2-methoxyethyl ammonium tetrafluoroborate. *J. Mol. Liq.* **2009**, *150*, 16–21.
- (26) Domańska, U.; Królikowski, M. Phase equilibria study of the binary systems (1-butyl-3-methylimidazolium tosylate ionic liquid + water, or organic solvent). *J. Chem. Thermodyn.* **2010**, *42*, 355–362.
- (27) Wu, B.; Zhang, Y.; Wang, H.; Yang, L. Temperature dependence of phase behavior for ternary systems composed of ionic liquid + sucrose + water. *J. Phys. Chem. B* **2008**, *112*, 13163–13165.
- (28) Wu, B.; Zhang, Y.; Wang, H. Phase behavior for ternary systems composed of ionic liquid + saccharides + water. *J. Phys. Chem. B* **2008**, *112*, 6426–6429.
- (29) Atkin, R.; Warr, G. G. Phase behavior and microstructure of microemulsions with a room-temperature ionic liquid as the polar phase. *J. Phys. Chem. B* **2007**, *111*, 9309–9316.
- (30) Anjum, N.; Guedeau-Boudeville, M. A.; Stubenrauch, C.; Mourchid, A. Phase behavior and microstructure of microemulsions containing the hydrophobic ionic liquid 1-butyl-3-methylimidazolium hexafluorophosphate. *J. Phys. Chem. B* **2009**, *113*, 239–244.
- (31) An, X.; Chen, J.; Huang, Y.; Shen, W. Coexistence curves of a critical microemulsion of AOT–water–octane. *J. Colloid Interface Sci.* **1998**, *203*, 140–145.
- (32) An, X.; Huang, Y.; Shen, W. Critical behaviour of {water + nonane + sodium di(2-ethyl-1-hexyl)sulphosuccinate} microemulsions. *J. Chem. Thermodyn.* **2002**, *34*, 1107–1116.
- (33) Peng, S.; An, X.; Shen, W. Critical phenomenon of nonaqueous microemulsion (AOT + DMA + decane). *J. Colloid Interface Sci.* **2005**, *287*, 141–145.
- (34) Martín, A.; López, I.; Monroy, F.; Casielles, A. G.; Ortega, F.; Rubio, R. G. Critical behavior of ionic micellar systems at different salt concentrations. *J. Chem. Phys.* **1994**, *101*, 6874–6879.
- (35) Aschauer, R.; Beysens, D. Critical behavior of a three-component microemulsion. *Phys. Rev. E* **1993**, *47*, 1850–1855.
- (36) Wagner, M.; Stanga, O.; Schröer, W. The liquid–liquid coexistence of binary mixtures of the room temperature ionic liquid 1-methyl-3-hexylimidazolium tetrafluoroborate with alcohols. *Phys. Chem. Chem. Phys.* **2004**, *6*, 4421–4431.
- (37) Schröer, W.; Wagner, M.; Stanga, O. Apparent mean-field criticality of liquid–liquid phase transitions in ionic solutions. *J. Mol. Liq.* **2006**, *127*, 2–9.
- (38) Schröer, W.; Vale, V. R. Liquid–liquid phase separation in solutions of ionic liquids: phase diagrams, corresponding state analysis and comparison with simulations of the primitive model. *J. Phys.: Condens. Matter* **2009**, *424119*, 1–21.
- (39) Dittmar, H.; Butka, A.; Vale, V. R.; Schröer, W. Liquid–liquid phase transition in the ionic solutions of tetra-n-butylammonium chloride in o-xylene and ethylbenzene: Phase diagrams and corresponding state analysis. *J. Mol. Liq.* **2009**, *145*, 116–128.
- (40) Lv, H.; Guo, Y.; An, X.; Shen, W. Liquid-liquid coexistence curves of {x1-butyl-3-methylimidazolium tetrafluoroborate + (1-x)1,3-propanediol} and {x1-butyl-3-methylimidazolium tetrafluoroborate + (1-x)1,4-butanediol}. *J. Chem. Eng. Data* **2010**, *55*, 2482–2488.
- (41) Kim, Y. W.; Baird, J. K. Reaction kinetics and critical phenomena: Rates of some first order gas evolution reactions in binary solvents with a consolute point. *J. Phys. Chem. A* **2005**, *109*, 4750–4757.
- (42) Clunie, J. C.; Baird, J. K. Suppression of the rate of hydrolysis of t-amylchloride at the consolute composition of isobutyric acid–water. *Fluid Phase Equilib.* **1998**, *150–151*, 549–557.
- (43) Baird, J. K.; Clunie, J. C. Critical slowing down of chemical reactions in liquid mixtures. *J. Phys. Chem. A* **1998**, *102*, 6498–6502.
- (44) Kim, Y. W.; Baird, J. K. Kinetics of S<sub>N</sub>1 reactions in binary liquid mixtures near the critical point of solution. *J. Phys. Chem. A* **2003**, *107*, 8435–8443.
- (45) Hu, B.; Baird, J. K. Reaction kinetics and critical phenomena: Iodination of acetone in isobutyric acid + water near the consolute point. *J. Phys. Chem. A* **2010**, *114*, 355–359.
- (46) Gao, Y.; Hilfert, L.; Voigt, A.; Sundmacher, K. Decrease of droplet size of the reverse microemulsion 1-Butyl-3-methylimidazolium tetrafluoroborate/Triton X-100/cyclohexane by addition of water. *J. Phys. Chem. B* **2008**, *112*, 3711–3719.